

## Sea Ice Thickness and Snow Depth Data Collected by Ship-based Video Observations during the 29th to 48th Japanese Antarctic Research Expeditions

Shotaro Uto<sup>1\*</sup>, Haruhito Shimoda<sup>1</sup>, Shigeru Aoki<sup>2</sup>, Shuki Ushio<sup>3</sup>, Fumihiko Nishio<sup>4</sup>  
Hiroyuki Wakabayashi<sup>5</sup>, Gen Hashida<sup>3</sup>, Kumiko Goto-Azuma<sup>3</sup>  
Atsushi Furusaki<sup>6</sup> and Kazutaka Tateyama<sup>7</sup>

<sup>1</sup> National Maritime Research Institute

6-38-1, Shinkawa, Mitaka city, Tokyo 181-0004.

<sup>2</sup> Institute of Low Temperature Science, Hokkaido University

Kita-19, Nishi-8, Kita-ku, Sapporo 060-0819.

<sup>3</sup> National Institute of Polar Research, Research Organization of Information and Systems

Kaga 1-chome, Itabashi-ku, Tokyo 173-8515.

<sup>4</sup> Center for Environmental Remote Sensing, Chiba University

1-33 Yayoi, Inage, Chiba 263-8522.

<sup>5</sup> College of Engineering, Nihon University

1 Naka-gawara, Tokusada, Tamura-machi, Koriyama, Fukushima 963-8642.

<sup>6</sup> Asahikawa National College of Technology

2-2-1-6, Shunkoudai, Asahikawa, Hokkaido 071-8142.

<sup>7</sup> Department of Civil and Environmental Engineering, Kitami Institute of Technology

165, Koen-cho, Kitami, Hokkaido 090-8507.

\*Corresponding author. E-mail: uto@nmri.go.jp

### Introduction

The Japanese Antarctic Research Expedition (hereafter denoted as JARE) initiated the ship-based video observations of sea ice and snow thicknesses in December 1987 (JARE-29, Kamimura and Kitagawa 1989).

A downward-looking video camera was mounted at the side deck of the Japanese Antarctic Research vessel, icebreaker “*Shirase*” for measuring sea ice and snow thicknesses during its outbound and homebound voyages ( to and from Syowa Station (69° 00' E, 39° 35' S)).

These observations had been conducted consecutively from December 1988 to January 1991 (JARE-30 to 32) as part of the Japanese Antarctic Climate Research (ACR) program. The results were reported by Shimoda *et. al* (1997).

After two periods of observation in December 1997 (JARE-39) and December 1999

(JARE-41), video observations have been conducted consecutively since December 2000 (JARE-42).

This report summarizes the results of ship-based video observations of sea ice and snow thicknesses from JARE-29 to 48.

### Method and accuracy

Fig. 1 shows the sea ice monitoring system onboard “*Shirase*” since December 2000. Ice and snow thickness are measured using a downward-looking video camera situated at the side deck. Ice is broken into pieces at the bow and a few of them turn into side-up positions. Using these images, ice and snow thicknesses can be measured along the vessel’s track (Fig. 2).

It is reported that this method has good accuracy for level and moderately deformed ice (Shimoda *et al.*, 1996, Lensu and Haas, 1998). Shimoda *et al.* (1996) conducted the uncertainty analysis of the measurement error for relatively thin ice in the Sea of Okhotsk. They concluded that the 95% confidence interval is within 11% for 1m-thick ice (Table 2).

Deformed ice such as ridged and hummocked ice often contains an unconsolidated part, which falls off by ice breaking process. Thus it is recognized that this method is not suitable for such highly deformed ice. This method is fundamentally suitable for the measurement of land fast ice in Lützw-Holm Bay, which Bay mostly consists of level and moderately deformed ice.

Uto *et al.* (2006) derived the following correlation equation of total thickness (=ice plus snow thickness) measured by the video and Electro-magnetic induction (EM) methods (see Fig. 1) using the concurrent measurement dataset in Lützw-Holm Bay.

$$Z_{I\_EM} = Z_{I\_Video} + 0.179 \times Z_{I\_Video}^2 \quad (1)$$

Here,  $Z_{I\_EM}$  and  $Z_{I\_Video}$  denote the total thickness by the EM and video methods, respectively. This equation indicates that the video method gives thinner total thickness than the EM method, the difference increases as the thickness.

It is observed that the thick multi-year, summer ice often contains the loose undermost layer, which falls off during turning into the side-up position (Uto *et al.*, 2006). It might cause the under-estimation of thickness for thick multi-year ice like highly deformed ice. The equation (1) supports that the video method gives the thickness of the consolidated part of thick multi year ice. Thus this equation might be helpful for correcting thickness measured by the video method to the overall thickness, if it is thick multi-year land fast ice including loose undermost layer.

## Results

Table 1. Summary of the video observations of ice and snow thicknesses

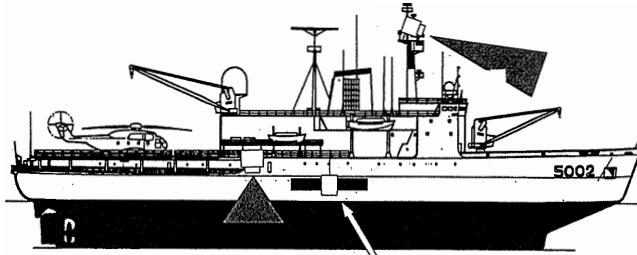
JARE	Voyage	Principal Observer	Date of Observation		No. of Data		Position Data
			from	to	Total Thickness	Snow Depth	
29	Outbound	Uto	1987/12/16	1988/1/1	130	48	Suzuki and Fukuchi(1997)
	Homebound		1988/2/3	1988/2/5	93	0	
30	Outbound	Endoh	1988/12/25	1988/12/29	729	0	Log book of Shirase
31	Outbound	Takizawa	1989/12/15	1990/1/10	5885	211	Log book of Shirase
32	Outbound	Ohshima	1990/12/15	1991/1/6	3089	0	Ohtaka, Private communication
39	Outbound	Aoki	1997/12/12	1998/1/25	264	54	Aoki, Private communication
41	Outbound	Ushio	1999/12/17	1999/12/24	181	50	Ushio, Private communication
42	Outbound	Uto	2000/12/23	2000/12/30	308	81	Dedicated GPS measurement
	Homebound		2001/1/22	2001/2/17	184	13	
43	Outbound	Nishio	2001/12/15	2001/12/23	504	51	Dedicated GPS measurement
	Homebound		2002/2/10	2002/2/12	85	8	
44	Outbound	Hashida	2002/12/15	2002/12/26	217	62	Dedicated GPS measurement
	Homebound	Wakabayashi	2003/2/10	2003/2/22	122	63	
45	Outbound	Azuma	2003/12/15	2003/12/21	463	189	Dedicated GPS measurement
46	Outbound	Furusaki	2004/12/15	2004/12/21	1496	949	Dedicated GPS measurement
	Homebound	Azuma	2005/2/9	2005/2/18	1553	603	
47	Outbound	Shimoda	2005/12/16	2005/12/24	598	134	Dedicated GPS measurement
	Homebound		2006/02/12	2006/02/12	80	22	
48	Outbound	Tateyama	2006/12/17	2006/12/23	686	236	Dedicated GPS measurement
	Homebound		2007/02/11	2007/02/19	544	185	

Table 2. Upper and lower values of the 95% confidence interval  
(Shimoda *et al.* 1996)

h (cm)	U+ (cm)	U- (cm)
10	2.05	2.13
20	2.34	2.63
30	2.76	3.30
40	3.26	4.05
50	3.89	5.82
60	4.49	6.86
70	5.11	7.92
80	5.74	8.99
90	6.38	10.06
100	7.03	11.14

U+ and U- give the upper and lower values of the 95% confidence interval, respectively.

Forward-looking Video  
(Ice Concentration)



Downward-looking Video  
(Ice and Snow Thickness)

EM and Laser  
(Total Thickness)

Fig. 1. Sea ice monitoring system onboard "Shirase" since December 2000.

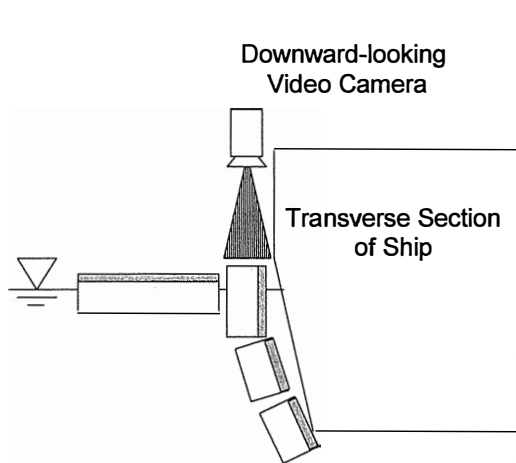


Fig. 2. Principle of ice and snow thickness measurement using a downward-looking video camera.

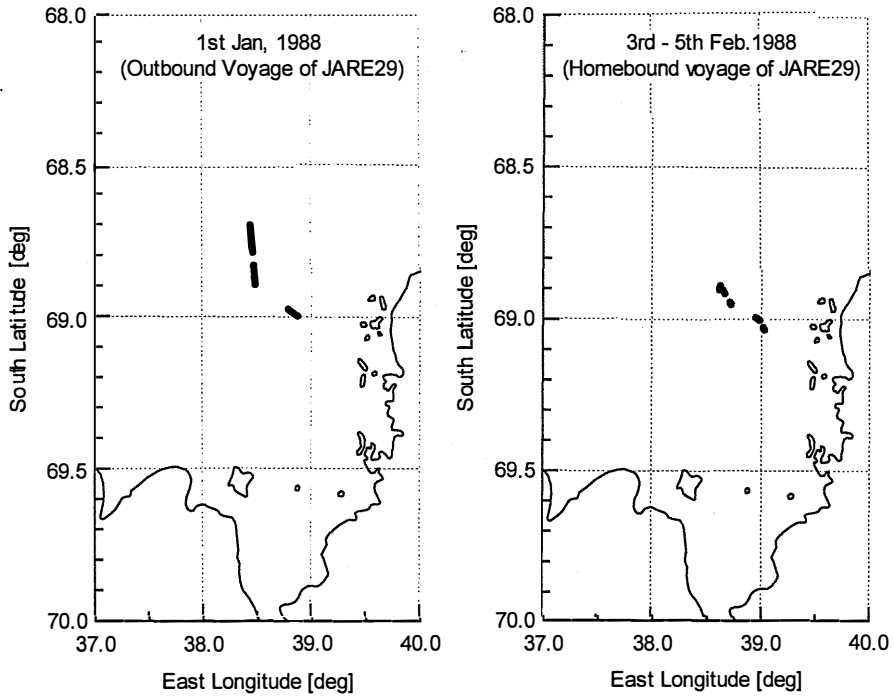


Fig. 3 (a) Locations of ice and snow thickness measurements of land-fast ice in Lützw-Holm Bay during the summer operations of JARE-29 (left : outbound voyage, right : homebound voyage).

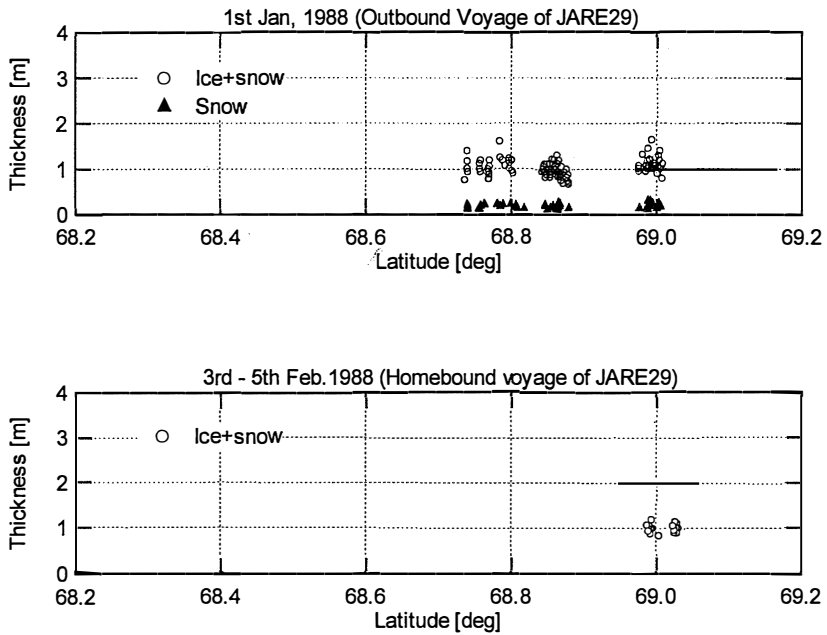


Fig. 3 (b) Ice and snow thickness distributions of land fast ice in Lützw-Holm Bay during the summer operation of JARE-29 (top : outbound voyage, bottom : homebound voyage).

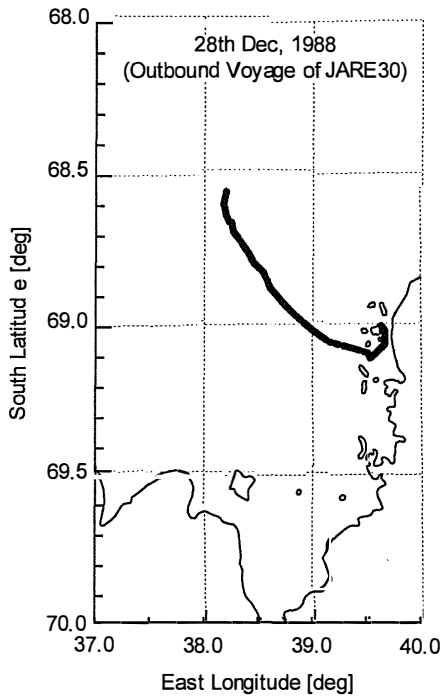


Fig. 4 (a) Locations of ice and snow thickness measurements of land-fast ice in Lützw-Holm Bay during the outbound voyage of the summer operations of JARE-30.

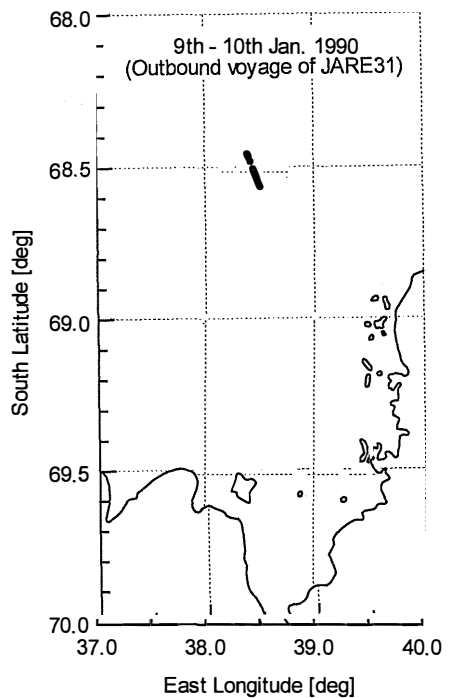


Fig. 5 (a) Locations of ice and snow thickness measurements of land-fast ice in Lützw-Holm Bay during the outbound voyage of the summer operations of JARE-31.

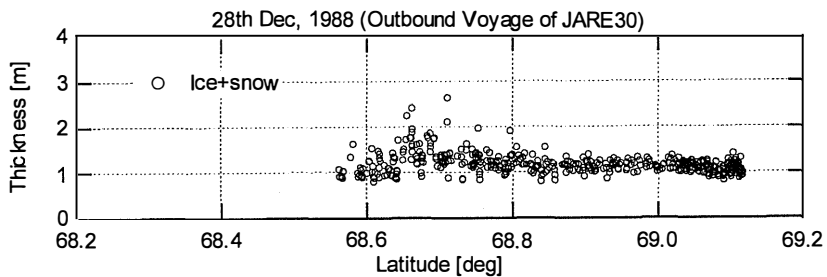


Fig. 4 (b) Ice and snow thickness distributions of land fast ice in Lützw-Holm Bay during the outbound voyage of the summer operations of JARE-30.

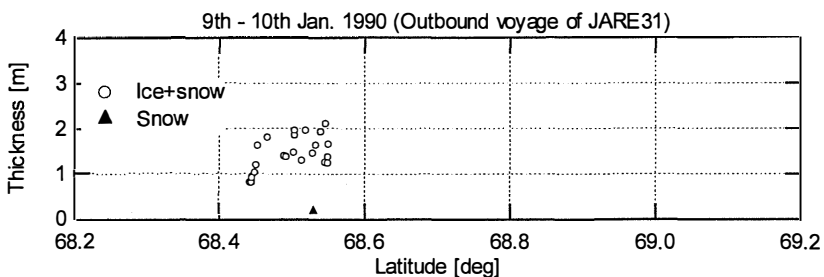


Fig. 5 (b) Ice and snow thickness distributions of land fast ice in Lützw-Holm Bay during the outbound voyage of the summer operations of JARE-31.

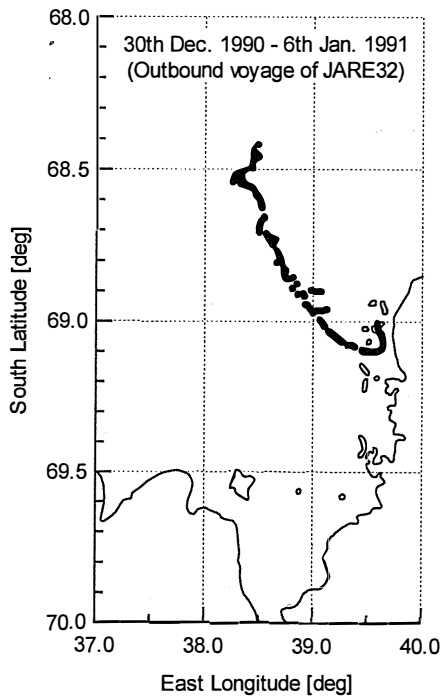


Fig. 6 (a) Locations of ice and snow thickness measurements of land-fast ice in Lützw-Holm Bay during the outbound voyage of the summer operations of JARE-32.

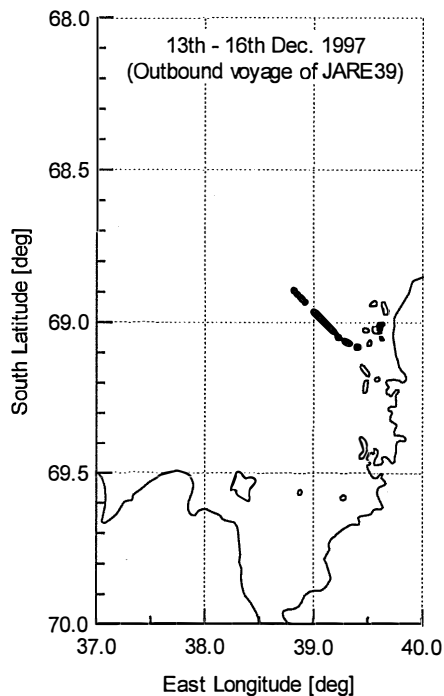


Fig. 7 (a) Locations of ice and snow thickness measurements of land-fast ice in Lützw-Holm Bay during the outbound voyage of the summer operations of JARE-39.

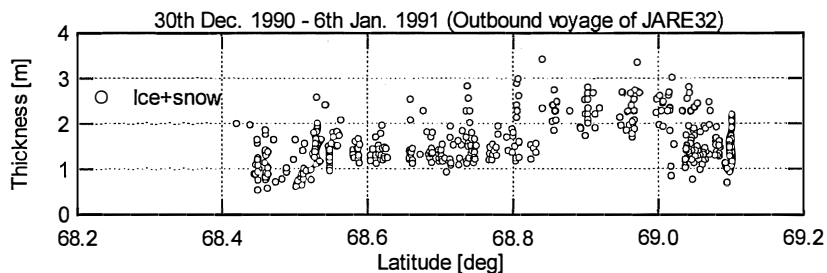


Fig. 6 (b) Ice and snow thickness distributions of land fast ice in Lützw-holm Bay during the outbound voyage of the summer operations of JARE-32.

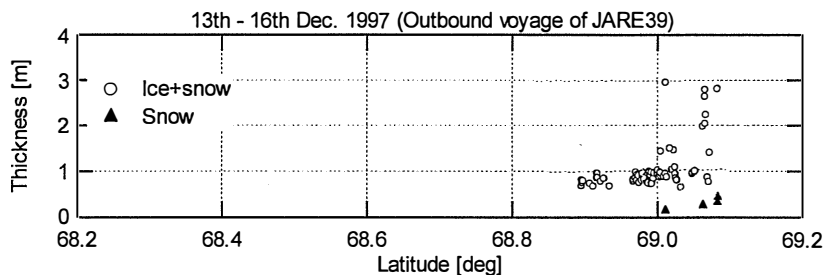


Fig. 7 (b) Ice and snow thickness distributions of land fast ice in Lützw-Holm Bay during the outbound voyage of the summer operations of JARE-39.

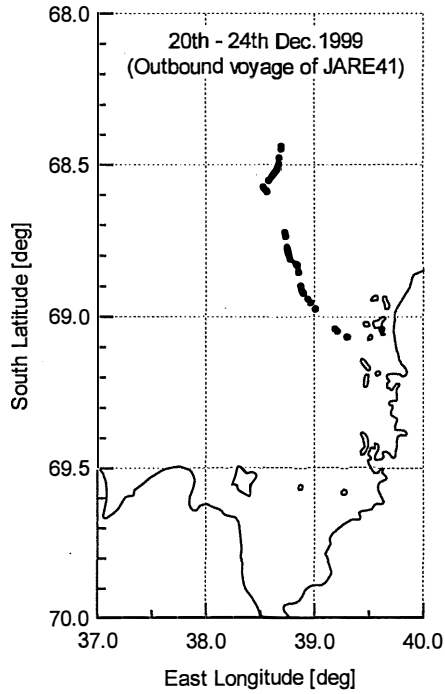


Fig. 8 (a) Locations of ice and snow thickness measurements of land-fast ice in Lützw-Holm Bay during the outbound voyage of the summer operations of JARE-41.

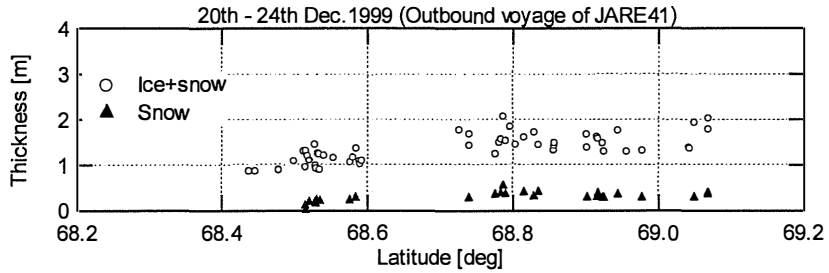


Fig. 8 (b) Ice and snow thickness distributions of land fast ice in Lützw-Holm Bay during the outbound voyage of the summer operations of JARE-41.



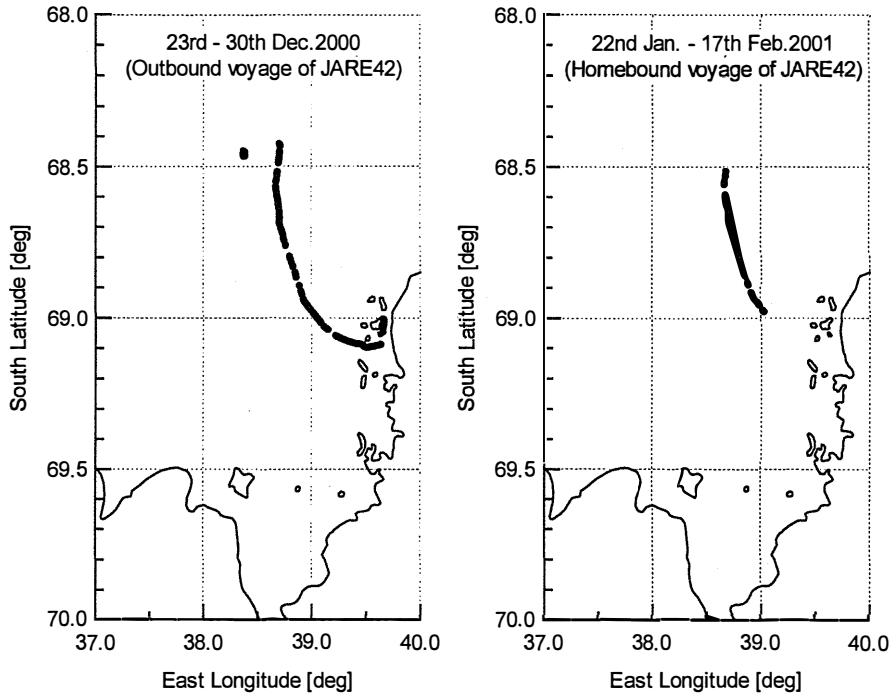


Fig. 9 (a) Locations of ice and snow thickness measurements of land-fast ice in Lützw-Holm Bay during the summer operations of JARE-42 (left : outbound voyage, right : homebound voyage).

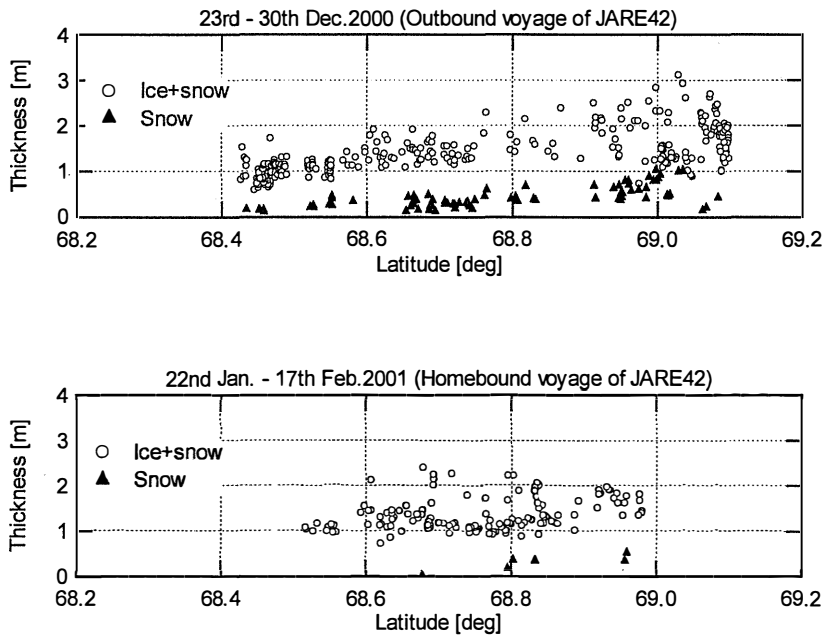


Fig. 9 (b) Ice and snow thickness distributions of land fast ice in Lützw-Holm Bay during the summer operations of JARE-42 (top : outbound voyage, bottom : homebound voyage).

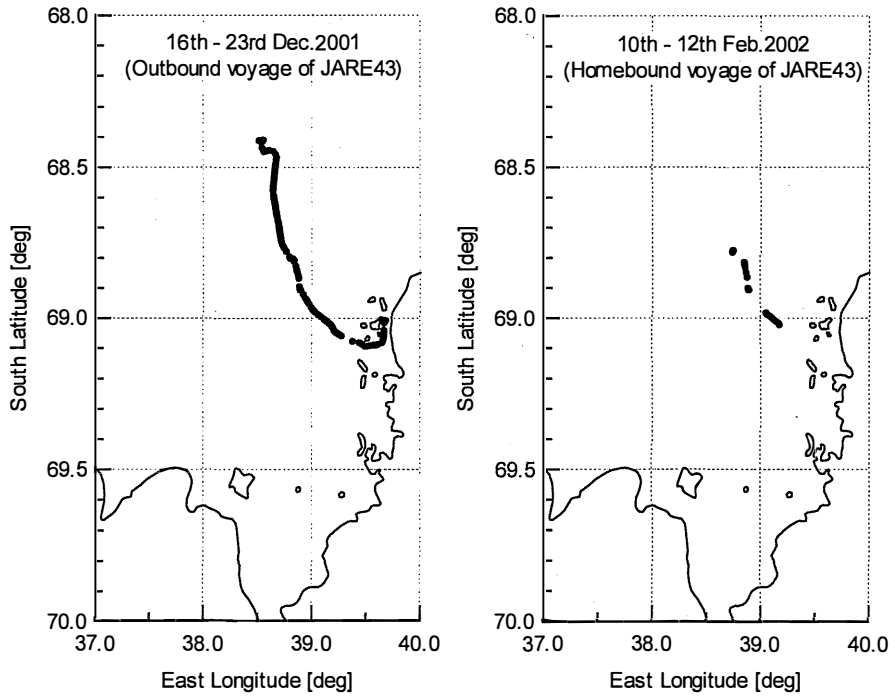


Fig. 10 (a) Locations of ice and snow thickness measurements of land-fast ice in Lützwahlm Bay during the summer operations of JARE-43 (left : outbound voyage, right : homebound voyage).

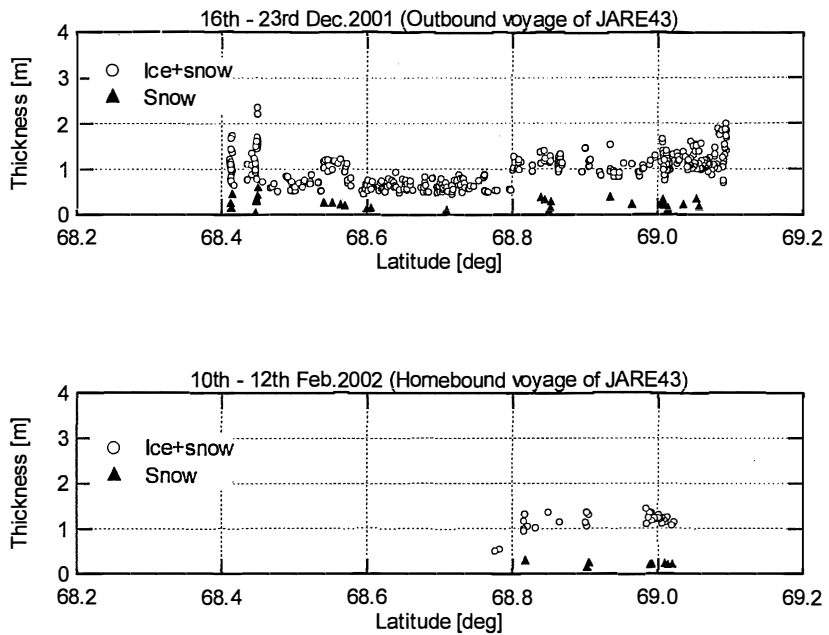


Fig. 10 (b) Ice and snow thickness distributions of land fast ice in Lützwahlm Bay during the summer operations of JARE-43 (top : outbound voyage, bottom : homebound voyage).

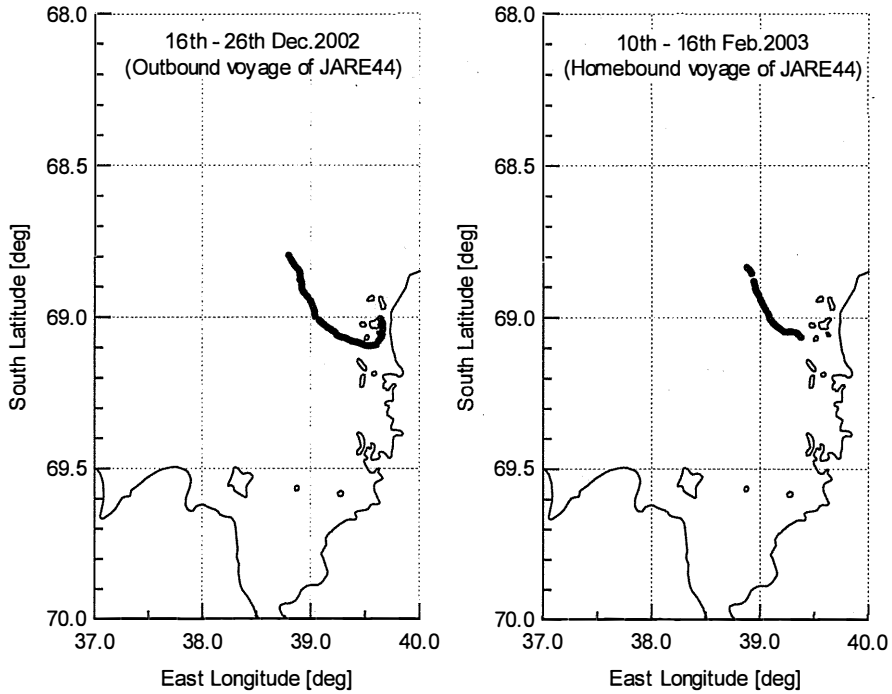


Fig. 11 (a) Locations of ice and snow thickness measurements of land-fast ice in Lützw-Holm Bay during the summer operations of JARE-44 (left : outbound voyage, right : homebound voyage).

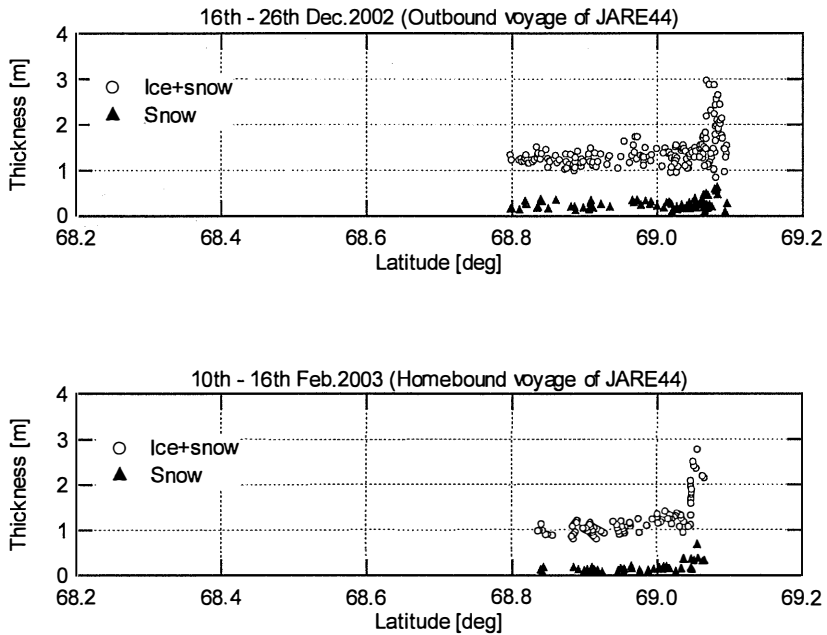


Fig. 11 (b) Ice and snow thickness distributions of land fast ice in Lützw-Holm Bay during the summer operations of JARE-44 (top : outbound voyage, bottom : homebound voyage).

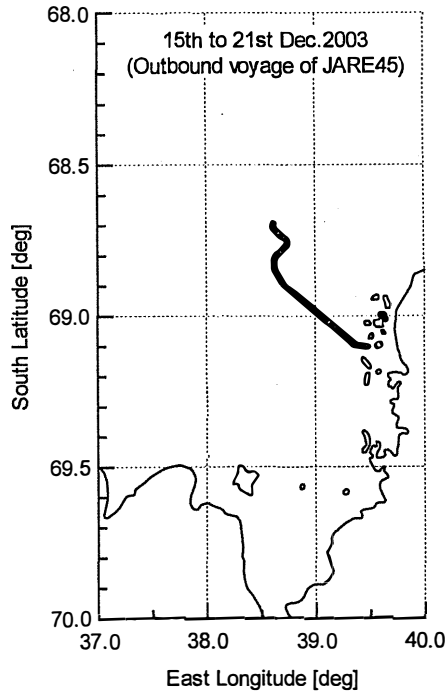


Fig. 12 (a) Locations of ice and snow thickness measurements of land-fast ice in Lützw-Holm Bay during the outbound voyage of the summer operations of JARE-45.

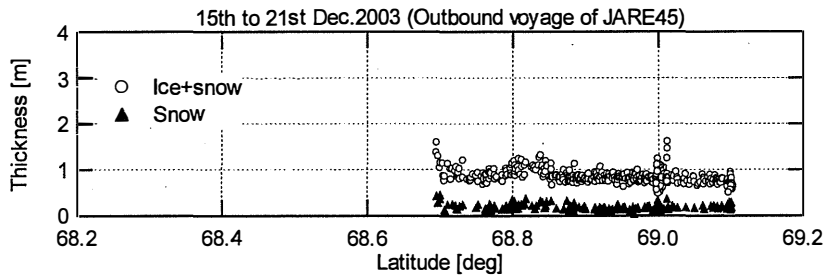


Fig. 12 (b) Ice and snow thickness distributions of land fast ice in Lützw-Holm Bay during the outbound voyage of the summer operations of JARE-45.

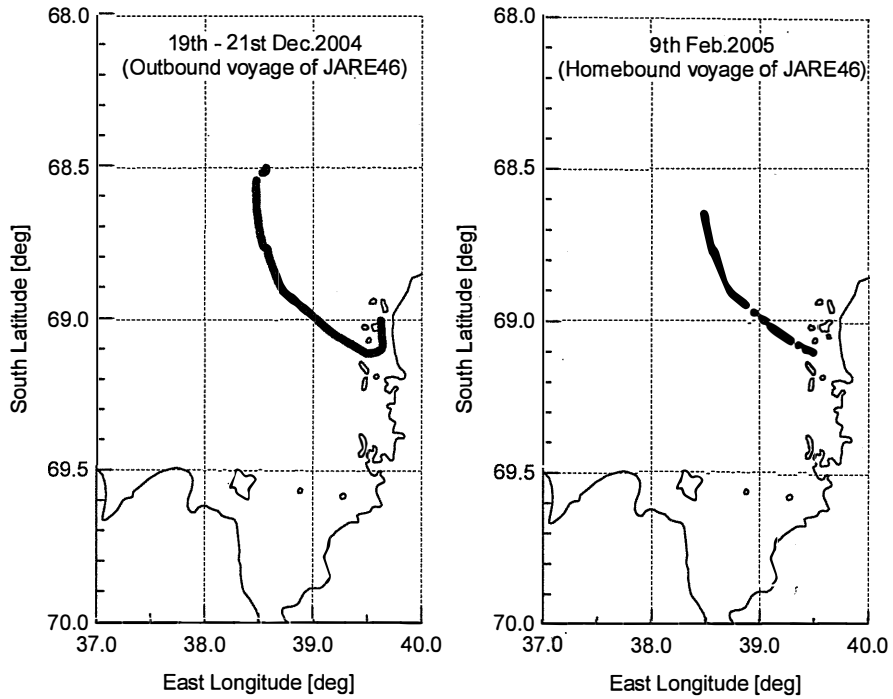


Fig. 13 (a) Locations of ice and snow thickness measurements of land-fast ice in Lützw-Holm Bay during the summer operations of JARE-46 (left : outbound voyage, right : homebound voyage).

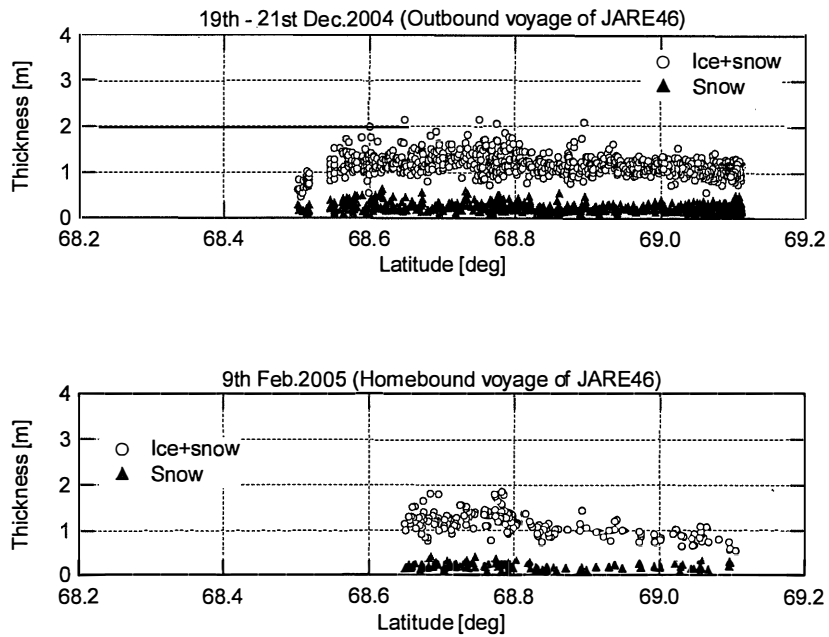


Fig. 13 (b) Ice and snow thickness distributions of land fast ice in Lützw-Holm Bay during the summer operations of JARE-46 (top : outbound voyage, bottom : homebound voyage).

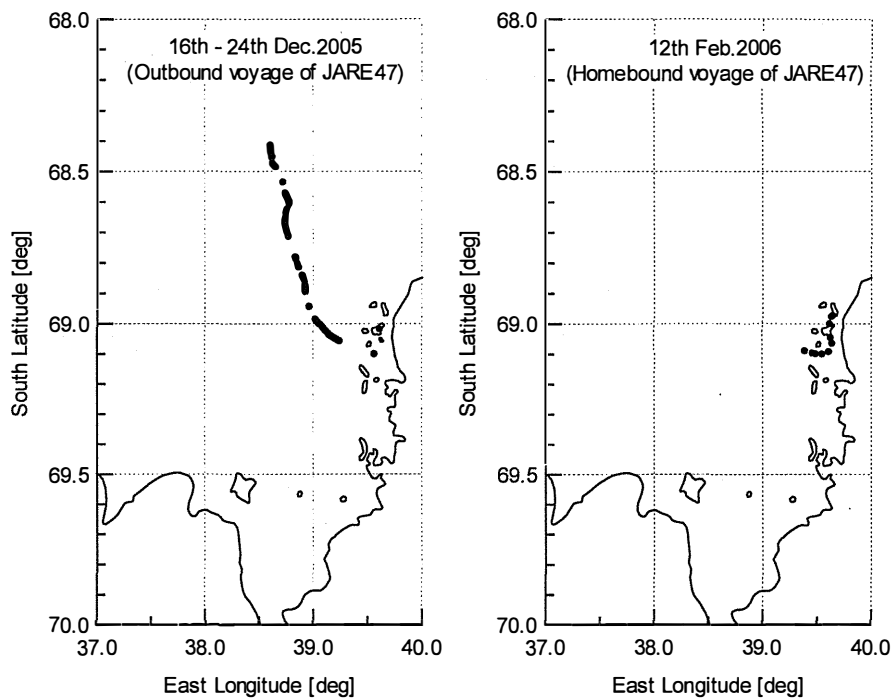


Fig. 14 (a) Locations of Ice and Snow Thickness Measurements of land-fast ice in Lützw-Holm Bay during the summer operations of JARE-47 (left : outbound voyage, right : homebound voyage).

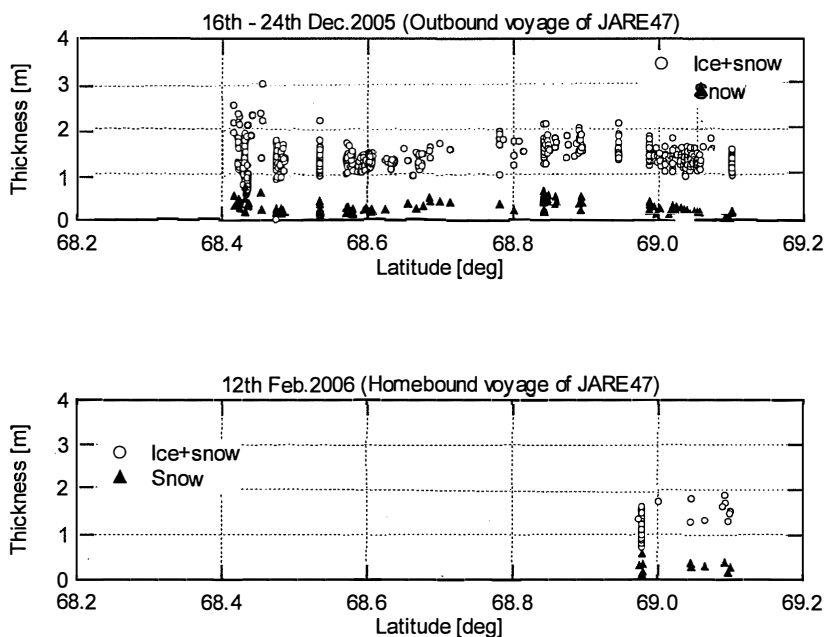


Fig. 14 (b) Ice and snow thickness distributions of land fast ice in Lützw-Holm Bay during the summer operations of JARE-47 (top : outbound voyage, bottom : homebound voyage).

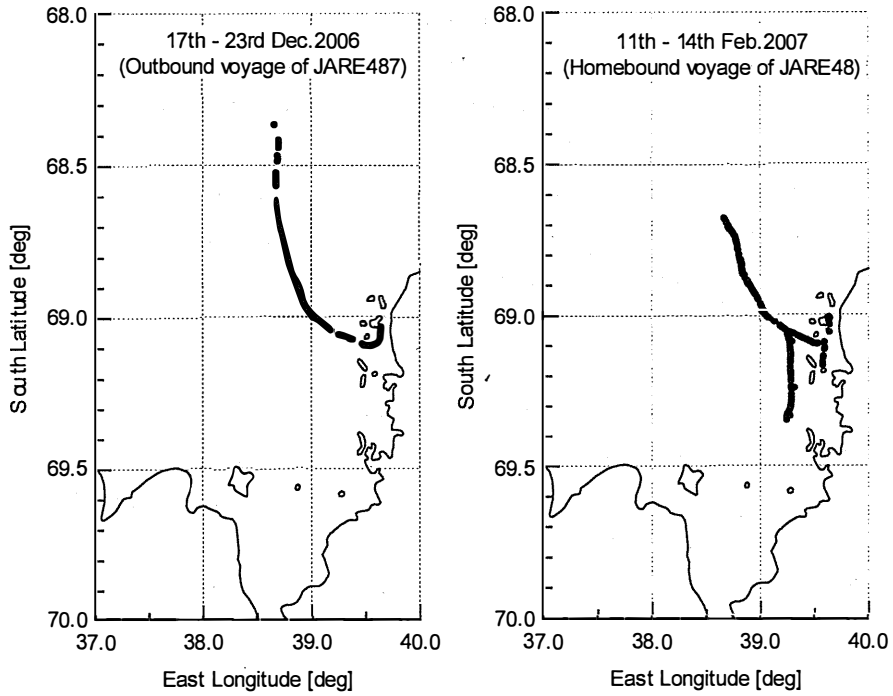


Fig. 15 (a) Locations of ice and snow thickness measurements of land-fast ice in Lützw-Holm Bay during the summer operations of JARE-48 (left : outbound voyage, right : homebound voyage).

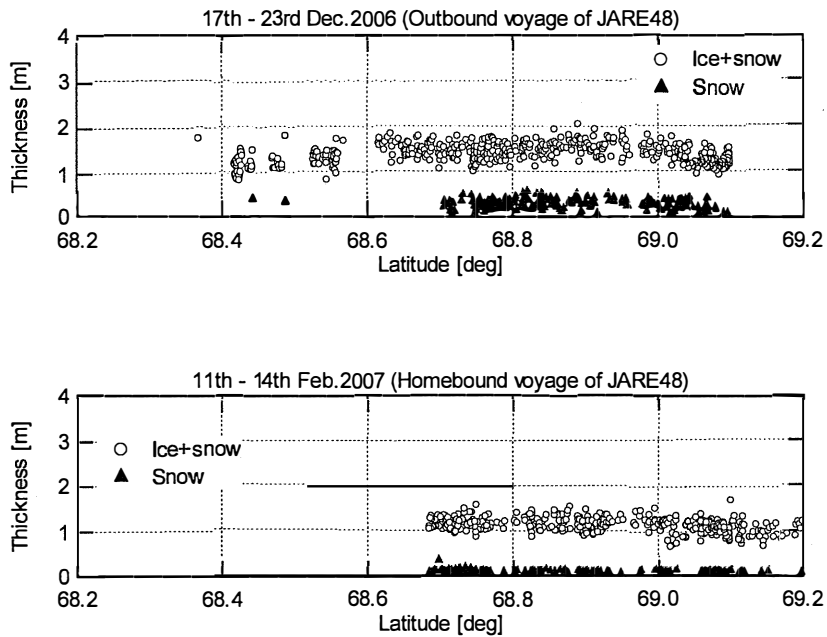


Fig. 15 (b) Ice and snow thickness distributions of land fast ice in Lützw-Holm Bay during the summer operations of JARE-48 (top : outbound voyage, bottom : homebound voyage).

### Publication

Archived data are accumulated and available *via* the Internet from the 'polar science data library system (POLARIS)' of the National Institute of Polar Research, Japan. Metadata in Japanese and English are available from :

[http://polaris.nipr.ac.jp/~dbase/300/300\\_data\(uto\).htm](http://polaris.nipr.ac.jp/~dbase/300/300_data(uto).htm) in Japanese

[http://polaris.nipr.ac.jp/~dbase/e/300/e/300\\_data\(uto\).htm](http://polaris.nipr.ac.jp/~dbase/e/300/e/300_data(uto).htm) in English

The digital data (MS EXCEL format) are available from :

[http://polaris.nipr.ac.jp/~dbase/300/300\\_data\(uto\).htm](http://polaris.nipr.ac.jp/~dbase/300/300_data(uto).htm)

### Acknowledgements

The authors express their sincere gratitude to Dr. Endoh, Dr. Takizawa and Prof. Ohshima, the principal investigators of the observations in JARE-30, 31 and 32, respectively. The members of JARE and crew of icebreaker *Shirase* are appreciated for their assistance in the observations. The authors also thank Ms. Enokihara and Mr. Nemoto for their effort of analyzing video images.

### References

- Kamimura, A. and Kitagawa, H. (1989): Full-scale measurement on board Antarctic research vessel "*Shirase*". 54th general meeting of the Ship Research Institute, 7-14 (in Japanese).
- Lensu, M. and Haas, C. (1998): Comparison of ice thickness from ship based video with field data. Ice in Surface Waters, Proceedings of the 14th International Symposium on Ice, Vol. 1, 225-230.
- Shimoda, H., Endoh, T., Muramoto, K., Ono, N., Takizawa, T., Ushio, S., Kawamura, T. and Ohshima, K.I. (1997): Observation of sea-ice conditions in the Antarctic coastal region using ship-board video cameras. *Nankyoku Shiryo* (Antarct. Rec.), **41**, 355-365 (in Japanese with English abstract).
- Shimoda, H., Uto, S., Tamura, K. and Narita, S. (1996): Sea ice situations in the Sea of Okhotsk off the coast of Hokkaido by on board ship observations. Abstracts of the 11th International Symposium on Okhotsk Sea and Sea Ice, 156-160 (in Japanese with English summary).
- Uto, S., Shimoda, H. and Ushio, S. (2006): Characteristics of sea ice thickness and snow depth distributions of the summer land-fast ice in Lützow-Holmbukta, East Antarctica. *Ann. Glaciol.*, **44**, 281-287.